Simulation of the steady state of oscillators in the time domain

Hans Georg Brachtendorf
Embedded Systems Laboratory
University of Applied Sciences
of Upper Austria
Email: brachtd@fh-hagenberg.at

Kai Bittner
Embedded Systems Laboratory
University of Applied Sciences
of Upper Austria
Email: Kai.Bittner@fh-hagenberg.at

Rainer Laur
Institute for Electromagnetic Theory
and Microelectronics
University of Bremen, Germany
Email: Laur@item.uni-bremen.de

***Abstract*—The numerical calculation of the limit cycle of oscillators with resonators exhibiting a high quality factor such as quartz crystals is a difficult task in the time domain. Time domain integration formulas introduce numerical damping which leads asympotically to erroneous limit cycles or spurious oscillations. The numerical problems for solving the underlying differential algebraic equations are studied in detail. Based on these results a class of novel integration formulas is derived and the results are compared with the well-known Harmonic Balance (HB) technique. The discretized system is sparser than that of the HB method, therefore easier to solve and slower run time.**

I. Introduction

In this paper several multistep integration formulas for the simulation of quartz crystal oscillators are investigated. The considerations are restricted to equidistant grid spaces though the same observations can be made on a non-equidistant mesh. The investigations show that known multistep schemes such as the Backward Differentation Formulas (BDF) are not suited for oscillators. These methods converge by employing a grid refinement only slowly towards the correct limit cycle, known as numerical damping or exhibit spurious oscillations. The problem is mathematically investigated and solved by a new family of BDF like methods.

Single and multistep integration formulas (IFs) are well-known in the literature and their properties are studied in various papers and textbooks. The following non-comprehensive list [1]–[5] gives an overview on the extensive literature in this field. Due to their robustness and ease of implementation, multistep methods are favored in the field of circuit simulation. Known results on multistep techniques are only summarized here when required for the understanding of the derivations in the subsequent sections. The author refers to the standard literature in this field, i.e. [1], [4], [5]. The numerical problems arising from finite difference schemes for oscillatory circuits were studied in [6]–[8]. The treatment here follows the investigation in [9]. For literature emphasizing the electronic background the reader is expeled e.g. to the book of Chua, Lin; Horneber and Vlach, Singhal [3], [10], [11]. The book of Brenan et al [12] deals with differential algebraic equations (DAE) with higher index. DAEs with higher index resulting from electronic circuits are investigated e.g. in [13]–[17]. For a description of the DASSL software package for solving DAEs up to an index of two the author refer also to the book of Brenan et al [12].

978-3-9810801-8-6/DATE12/©2012 EDAA

II. Multistep integration formulas

This section gives an overview of known results on multistep methods which are required in the subsequent sections, and introduces also the nomenclature.

A system of uniquely solvable ordinary differential equations (ODE) of dimension m

$$\dot{x} = f(x,t), \quad x(0) = x_0, \quad f : \mathbb{R}^m \times \mathbb{R} \to \mathbb{R}^m \tag{1}$$

is considered. Let $\Phi(t_n, 0, x_0)$ be the exact solution of the ODE at timepoint t_n for the initial condition $x(0) = x_0$ and $\hat{x}_n(x_0)$ the numerical approximation. Further, let $\Delta t = t_n - t_{n-1}$ be the time step of the integration formula which is assumed to be constant in the sequel. An integration formula is convergent if for any uniquely solvable initial value problem $\dot{x} = f(x,t)$, $x(0) = x_0$ the global error vanishes for a vanishing time step $\lim_{\Delta t \to 0} ||\epsilon^G(t_n)|| = 0$, wherein $\epsilon^G(t_n) := \Phi(t_n, 0, x_0) - \hat{x}_n(x_0)$.

The global error is in general difficult to estimate. A necessary condition for global convergence is a vanishing local error $\epsilon^L(t_n) := \Phi(t_n, t_{n-1}, x_{n-1}) - \hat{x}_n(x_{n-1})$. An integration formula is consistent, if $\lim_{\Delta t \to 0} ||\frac{\epsilon^L(t_n)}{\Delta t}|| = 0$. The IFs are classified according to the order p with which the local discretization error vanishes for a vanishing time step

$$||\epsilon^L(t_n)|| < L \cdot \Delta t^{p+1}$$

wherein the constant L is independent of the time step Δt. Employing the short hand $x_{n+i} := \hat{x}(t_n + i\,\Delta t)$, $i \in \mathbb{Z}$ the multistep methods take the form

$$\sum_{i=0}^{k+1} a_i \; x_{n+1-i} = \Delta t \; \sum_{i=0}^{k+1} b_i \; f(x_{n+1-i}, t_{n+1-i}), \quad b_0 = 1 \tag{2}$$

Commercial circuit simulators employ often the single step trapezoidal method or the multistep BDFs. The trapezoidal method is unfortunately not suited for DAEs of an index larger than one and often exhibits spurious oscillations. The BDF-p formulas of consistency order p choose the $2k+3$ coefficients

a_i, b_i in such a way that the solution x_{n+1} is exact if $x(t)$ is a polynomial of degree p. We note here that the order of consistency is also of order p [3], [4]. From the above it follows that $2k+3 \geq p+1$. The class of BDF methods of consistency order p are defined as

$$\sum_{i=0}^{p} a_i \; x_{n+1-i} = \Delta t \cdot f(x_{n+1}, t_{n+1}) \tag{3}$$

The coefficents a_i of the 6 stable BDF methods are summarized in Table I. The special case $p = 1$ corresponds to the Backward Euler scheme.

TABLE I
COEFFICIENTS OF THE BDF METHODS FOR THE STABLE METHODS $p = 1, \ldots, 6$ [3].

order p	a_0	a_1	a_2	a_3	a_4	a_5	a_6
$p=1$	1	-1	0	0	0	0	0
$p=2$	$\frac{3}{2}$	-2	$\frac{1}{2}$	0	0	0	0
$p=3$	$\frac{11}{6}$	-3	$\frac{3}{2}$	$-\frac{1}{3}$	0	0	0
$p=4$	$\frac{25}{12}$	-4	3	$-\frac{4}{3}$	$\frac{1}{4}$	0	0
$p=5$	$\frac{137}{60}$	-5	5	$-\frac{10}{3}$	$\frac{5}{4}$	$-\frac{1}{5}$	0
$p=6$	$\frac{147}{60}$	-6	$\frac{15}{2}$	$-\frac{20}{3}$	$\frac{15}{4}$	$-\frac{6}{5}$	$\frac{1}{6}$

Consistency of the integration formula is a necessary but not a sufficient condition for the global convergence of the integration formula. Indeed, the propagation of the numercial error must be bounded for guaranteeing convergence which is referred to as the stability of the integration formula. For the investigation of the stability a homogeneous and linear test initial value problem of the form

$$\dot{x} = \lambda \; x, \; x(0) = 1, \; \lambda \in \mathbb{C} \tag{4}$$

is common practice. The eigenvalue $\lambda \in \mathbb{C}$ is a free parameter. Employing a multistep method (2) leads to the difference equation

$$\sum_{i=0}^{k+1} a_i \; x_{n+1-i} - \sigma \; \sum_{i=0}^{k+1} b_i \; x_{n+1-i} = 0, \; b_0 = 1, \; \sigma := \Delta t \, \lambda \in \mathbb{C} \tag{5}$$

Applying the z-transform to (5) one obtains the characteristic polynomial of the difference equation

$$P(z) = \sum_{i=0}^{k+1} a_i \; z^{k+1-i} - \sigma \; \sum_{i=0}^{k+1} b_i \; z^{k+1-i}, \quad b_0 = 1, \quad z \in \mathbb{C} \tag{6}$$

An integration formula is absolutely stable for a fixed time step Δt, if all $k+1$ roots z_i of the characteristic polynomial $P(z)$ fulfill one of the following conditions

$$\begin{aligned} |z_i| &< 1 \\ |z_i| &= 1 \quad \text{only if the root is of single order.} \end{aligned}$$

The stability depends obviously on the chosen timestep. Values of $\sigma = \Delta t \; \lambda$ for which the roots fulfill the requirements are referred to as regions of absolute stability. Moreover every absolutely stable and consistent mutistep method is convergent. A multistep method is A-stable, if the range of convergence comprises the left half-plane and stiffly stable, if all roots of the characteristic polynomial $P(z)$ fulfill the requirement

$$\lim_{\sigma \to \infty} |z_i| = 0, \quad 1 \leq i \leq k+1$$

The BDF methods are by construction stiffly stable and A-stable for $p = 1, 2$ whereas the trapezoidal method is only A-stable. The range of absolute stability of the BDF-2 is plotted in Fig. 1.

III. DIFFERENCE SCHEMES FOR THE STEADY STATE ANALYSIS

In this section the discretization of the periodic steady state of autonomous circuits described by the system of DAEs

$$f(x(t), \dot{x}(t)) = i(x(t)) + \frac{\mathrm{d}}{\mathrm{d}t} \, q(x(t)) = 0, \quad x(T) - x(0) = 0 \tag{7}$$

with multistep schemes are investigated on an equidistant mesh. The discretization of the ordinary DAEs by finite differences leads to circulant difference schemes. In that case, the eigenvalues and eigenvectors can be calculated directly employing the Discrete Fourier Transform (DFT). For ease of comparison with the Harmonic Balance (HB) method a mesh with $2K+1$ gridpoints is chosen. Hence, the grid spacing is $\Delta t = \frac{T}{2K+1}$, wherein $T = \frac{1}{f_0}$ is the period of the waveform. Without loss of generality we assume $t_0 = 0$ and $t_n = n \cdot \Delta t$, $n \in \mathbb{N}$. Employing e.g. the Backward Euler's scheme and using of the periodicity constraint, the following difference operator is obtained

$$\nabla_{BE} = \frac{1}{\Delta t} \begin{pmatrix} 1 & & & & -1 \\ -1 & \ddots & & & \\ & \ddots & \ddots & & \\ & & \ddots & \ddots & \\ & & & -1 & 1 \end{pmatrix} \tag{8}$$

Likewise, a central difference scheme leads to the difference operator

$$\nabla_{CD} = \frac{1}{2 \, \Delta t} \begin{pmatrix} 0 & 1 & & & -1 \\ -1 & \ddots & \ddots & & \\ & \ddots & \ddots & \ddots & \\ & & \ddots & \ddots & 1 \\ 1 & & & -1 & 0 \end{pmatrix} \tag{9}$$

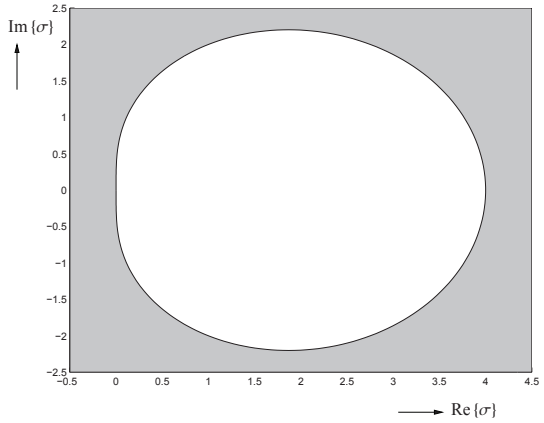

(a) Region of absolute stability of the BDF-2 method.

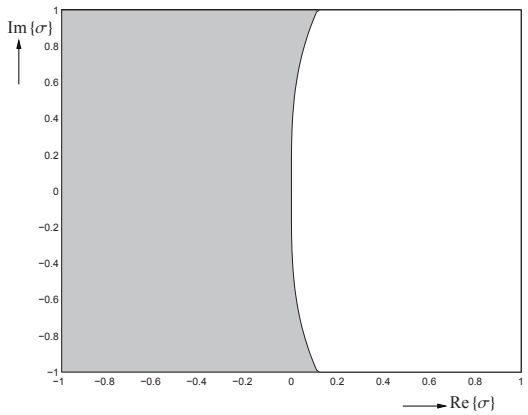

(b) Region of stability of the BDF-2 method (cutout).

Fig. 1. Regions of absolute stability of the BDF formula $p = 2$ (grey area). The range of convergence covers the left half plane (A-stability).

It is easily verified that the discretization error is in $O(\Delta t)$ for the Euler method (8) and $O(\Delta t^2)$ for the central difference scheme (9), sufficient differentiability of the signals presupposed. The schemes (8 and 9) are circulant matrices, the eigenvectors coincide therefore with the column vectors of the inverse DFT ($\jmath = \sqrt{-1}$)

$$x_k = \left[\mathrm{e}^{-\jmath\, k \cdot \frac{2\pi\, K}{2K+1}}, \ldots, \mathrm{e}^{\jmath\, k \cdot \frac{2\pi\, l}{2K+1}}, \ldots, \mathrm{e}^{\jmath\, k \cdot \frac{2\pi\, K}{2K+1}}\right]^T, \; |k| \leq K \tag{10}$$

After the discretization of the periodic waveforms they can be expanded in a basis spanned by the eigenvectors x_k. It is readily verified that the eigenvalues of Euler's method (8) are given by

$$\lambda_k = \frac{1}{\Delta t}\left(1 - \mathrm{e}^{-\jmath\, k \cdot \frac{2\pi}{2K+1}}\right), \; |k| \leq K \tag{11}$$

and for the central difference scheme (9) by

$$\lambda_k = \jmath \frac{1}{\Delta t}\, \sin\left(k \cdot \frac{2\pi}{2K+1}\right), \; |k| \leq K \tag{12}$$

A Taylor series expansion of (11) and (12) results at low frequencies $k \ll K$ in the approximation $\lambda_k \approx \jmath\, k\, \frac{2\pi}{T}$. At low frequencies or on a fine grid the eigenvalues of both the difference schemes and the HB technique converge. The difference scheme ∇ is uniquely defined by its first column vector. Therefore the following notation is employed for further analysis

$$\nabla = \frac{1}{\Delta t}\, \mathrm{circ}(a_0, a_1, \ldots, a_{2K}) \tag{13}$$

wherein the coefficients a_i are the coefficients of the first column vector of ∇. The eigenvalues corresponding to the eigenvectors (10) are easily calculated by

$$\lambda_k = \frac{1}{\Delta t} \sum_{l=0}^{2K} a_l\, \mathrm{e}^{-\jmath\, \frac{2\,\pi\, k\, l}{2K+1}}, \quad -K \leq k \leq K \tag{14}$$

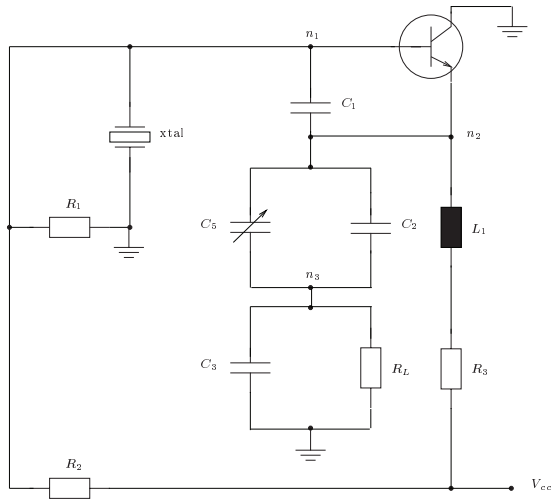

Fig. 2. Schematic of a 3 MHz Colpitts quartz crystal oscillator test circuit.

IV. Multistep methods for the calculation of limit cycles

The Fig. 2 shows as benchmark circuit a 3 MHz Colpitts oscillator with a quartz crystal. Due to their high quality factors, quartz crystals are well-suited as test examples for numerical methods because they are highly sensitive with regard to numerical damping effects [6], [9]. In what follows the reference solution of the limit cycle is obtained via the HB technique.

The Fig. 3 compares the numerically calculated limit cycles of a 3 MHz Colpitts oscillator employing 128 equally spaced mesh points for the Harmonic Balance technique (straight) and the BDF scheme of order $p = 2$ (dashed). The coefficients of the circulant operator (13) are given in table I. Due to the intrinsic numerical damping of the BDF-2 method, and even worse for the backward Euler method, these multistep methods

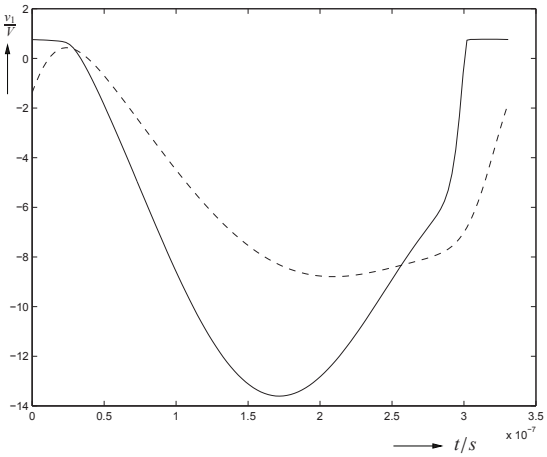

Fig. 3. Comparison of the numerically obtained limit cycle employing the second order BDF method (dashed) versus Harmonic Balance (straight), for a mesh of 128 grid points per period for the 3 MHz Colpitts oscillator depicted in Fig. 2.

are not suited for oscillators with a high-Q resonator. The numerically obtained amplitudes are significantly smaller than those calculated by HB. Furthermore, the numerical damping effect is only slowly diminishing by a grid refinement. Therefore the BDF-2 method is not suited for oscillator simulations. The reason can be explained by considering the range of absolute convergence of the BDF-2 method as depicted in Fig. 1. The imaginary axis belongs to the range of absolute stability and so regions of the right half-plane. Linearizing the oscillators at the operating point, there is essentially one complex conjugate pair of generalized eigenvalues of the variational problem with a small positive real part and large imaginary part. The normalized eigenvalue $\sigma = \Delta t\,\lambda$ lies therefore often in the range of absolute stability of the BDF-2 method, resulting into a pseudo numerically stable operating point though it is unstable in reality. The distance between σ, which depends on the step size Δt, and the border of absolute stability is a measure for the numerical damping. Though the distance vanishes for $\sigma \to 0$, i.e. small time steps, the BDF-2 method is completely run-time inefficient[1]. An alternative view on the numerical damping problem can be taken by analyzing the eigenvalues (14) of the BDF-2 formula

$$\Delta t\,\lambda_k = \frac{3}{2} - 2\mathrm{e}^{-\jmath\,\frac{2\pi k}{2K+1}} + \frac{1}{2}\mathrm{e}^{-2\,\jmath\,\frac{2\pi k}{2K+1}} \tag{15}$$

Using the short hand $z := \frac{2\pi}{2K+1}$ one obtains for the eigenvalue of the fundamental harmonic

$$\begin{aligned}\Delta t\,\lambda_{\pm 1} = \frac{3}{2} &- 2\left(\cos(\pm z) - \jmath\sin(\pm z)\right)\\ &+ \frac{1}{2}\left(\cos(\pm 2\,z) - \jmath\sin(\pm 2\,z)\right)\end{aligned}$$

[1]The range of convergence of the trapezoidal method coincides with the imaginary axis and does therefore not exhibit numerical damping. However the disadvantages of this integration formula has already been discussed above.

The real part of $\Delta t\,\lambda_{\pm 1}$ can be expanded into a Taylor series

$$\begin{aligned}\Delta t\ \mathrm{Re}\left\{\lambda_{\pm 1}\right\} &= \frac{3}{2} - 2\,\left(1 - \frac{z^2}{2!} + \frac{z^4}{4!} + O(z^6)\right)\\ &\quad + \frac{1}{2}\,\left(1 - \frac{4\,z^2}{2!} + \frac{16\,z^4}{4!} + \mathcal{O}(z^6)\right)\\ &= \frac{6\,z^4}{4!} + \mathcal{O}(z^6)\ >\ 0\end{aligned}$$

This means, that the BDF-2 formula leads due to the non-vanishing real part to a numerical damping effect and therefore to a loss of energy. The differential operator of the HB technique on the other hand has by construction solely imaginary eigenvalues.

Difference schemes employing a central difference scheme such as (9) exhibit only imaginary eigenvalues. One expects therefore a numerically better behavior when calculating the limit cycles of oscillators. This can be justified for our test example as illustrated in Fig. 4. The central difference scheme however leads to spurious oscillations or ringing. For a grid refinement the amplitude of the artifical ringing slowly disappears and its frequency increases.

V. Difference schemes exhibiting small numerical damping

The investigations of the previous section have shown that the intrinsic numerical damping of the BDF-2 scheme leads to erroneous results when applied to autonomous circuits such as oscillators. The same observation can be made for all BDF-p schemes. The trapezoidal method on the other hand is not suited for DAEs with a higher index.

In this section modified BDF methods are presented, which are well suited for systems exhibiting oscillatory behavior. For modified Adams methods the reader is referred to the work of Gautschi [18].

The BDF methods calculate the exact waveform if the signal can be represented by a polynomial of low degree. The modified BDF techniques proposed here calculate the exact solution if the waveform is represented by a trigonometric polynomial of low order. The coefficients a_i of the difference operator ∇ are calculated such that the eigenvalues (14) do not have a real part and therefore no numerical damping at low frequencies $-L \le k \le L$ occurs.

$$\lambda_k = \frac{1}{\Delta t}\sum_{l=0}^{p} a_l\,\mathrm{e}^{-\jmath\,\frac{2\,\pi\,k\,l}{2K+1}} = j\,k\,\frac{2\,\pi}{T},\ a_l = 0\ \forall\ l > p,\ |k| \le L \tag{16}$$

From (16) it follows readily that $p+1 \ge 2L+1$. The eigenvalues at low frequencies coincide therefore with the Harmonic Balance technique. The approximation of the derivative is therefore exact if the solution is a trigonometric polynomial of low degree. In what follows the special case of the identity $p+1 = 2L+1$ is considered. Again, employing the short hands $z := \frac{2\pi}{2K+1}$ and $w_K := \mathrm{e}^{-\jmath\,z}$ one gets from the equations (16)

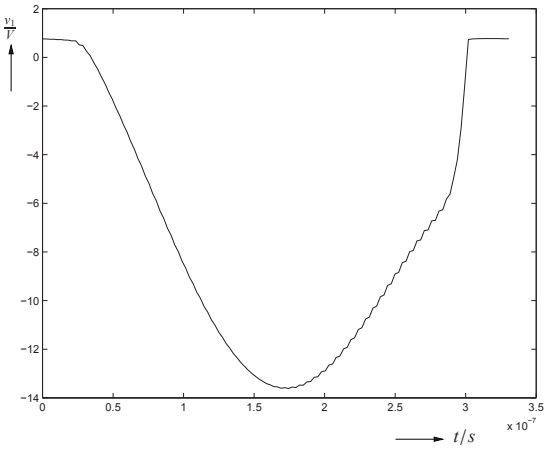

(a) Numerically calculated limit cycle at node 1 of the quartz oscillator Fig. 2.

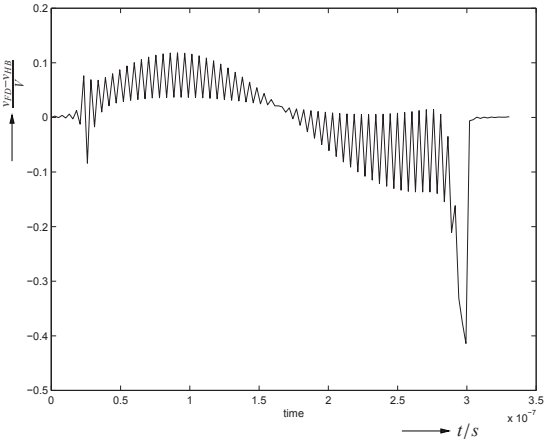

(b) Difference between the Harmonic Balance and central difference scheme solution at 1 of the test example Fig. 2.

Fig. 4. Comparison of the numerically calculated limit cycle between a central difference scheme and the Harmonic Balance method for 128 mesh points per period for the 3 MHz Colpitts quartz crystal oscillator depicted in Fig. 2.

the set of linear equations for calculating the coefficients a_i

$$\begin{pmatrix} w_K^0 & w_K^{-L} & \cdots & w_K^{-L(2L)} \\ \vdots & \vdots & \vdots & \vdots \\ w_K^0 & w_K^{l} & \cdots & w_K^{l(2L)} \\ \vdots & \vdots & \vdots & \vdots \\ w_K^0 & w_K^{L} & \cdots & w_K^{L(2L)} \end{pmatrix} \begin{pmatrix} a_0 \\ a_1 \\ \vdots \\ a_p \end{pmatrix} = \begin{pmatrix} -\jmath\, L\, z \\ \vdots \\ \jmath\, L\, z \end{pmatrix} \tag{17}$$

Because for even p every equation in (17) has a conjugate complex counterpart, all coefficients a_i are real. The method is illustrated for the cases $p = 2$ and $p = 4$.

$p = 2$:

$$\begin{pmatrix} 1 & 1 & 1 \\ 1 & \mathrm{e}^{-\jmath z} & \mathrm{e}^{-2\jmath z} \\ 1 & \mathrm{e}^{\jmath z} & \mathrm{e}^{2\jmath z} \end{pmatrix} \begin{pmatrix} a_0 \\ a_1 \\ a_2 \end{pmatrix} = \begin{pmatrix} 0 \\ \jmath z \\ -\jmath z \end{pmatrix}$$

By a simple reformulation one gets the system of equations with real matrix coefficients and real right hand side

$$\begin{pmatrix} 1 & 1 & 1 \\ 1 & \cos z & \cos 2z \\ 0 & -\sin z & -\sin 2z \end{pmatrix} \begin{pmatrix} a_0 \\ a_1 \\ a_2 \end{pmatrix} = \begin{pmatrix} 0 \\ 0 \\ z \end{pmatrix}$$

The solution is given by

$$\begin{pmatrix} a_0 \\ a_1 \\ a_2 \end{pmatrix} = \begin{pmatrix} z\,\dfrac{\cos z - \cos 2z}{\sin 2z - 2\sin z} & z\,\frac{\sin z}{\cos z - 1} & z\,\frac{1}{2\sin z} \end{pmatrix}^T$$

$p = 4$:

$$\begin{pmatrix} 1 & 1 & 1 & 1 & 1 \\ 1 & \mathrm{e}^{-\jmath z} & \mathrm{e}^{-2\jmath z} & \mathrm{e}^{-3\jmath z} & \mathrm{e}^{-4\jmath z} \\ 1 & \mathrm{e}^{\jmath z} & \mathrm{e}^{2\jmath z} & \mathrm{e}^{3\jmath z} & \mathrm{e}^{4\jmath z} \\ 1 & \mathrm{e}^{-2\jmath z} & \mathrm{e}^{-4\jmath z} & \mathrm{e}^{-6\jmath z} & \mathrm{e}^{-8\jmath z} \\ 1 & \mathrm{e}^{2\jmath z} & \mathrm{e}^{4\jmath z} & \mathrm{e}^{6\jmath z} & \mathrm{e}^{8\jmath z} \end{pmatrix} \begin{pmatrix} a_0 \\ a_1 \\ a_2 \\ a_3 \\ a_4 \end{pmatrix}$$
$$= \begin{pmatrix} 0 & \jmath z & -\jmath z & 2\jmath z & -2\jmath z \end{pmatrix}^T$$

It can moreover be shown that the modified BDF schemes are consistent. The Fig. 5(a) compares the simulated steady state by the modified BDF scheme of order $p = 2$ and the Harmonic Balance technique for the test circuit depicted in Fig. 2 at node 1 for a mesh of 128 grid points. Both simulations are in good agreement and the waveforms practically coincide (Fig. 5(b)). This contrasts to Fig. 3 where due to the numerical damping of the BDF-2 scheme both solutions differ significantly. The modified BDF-2 method can be implemented much easier than HB on the one hand. On the other hand this method leads to much sparser systems of equations when employing Newton like methods and moreover the condition number of the linearized system of equations is generally smaller. Therefore this modified BDF scheme is better suited compared with HB. For the solution of the resulting linear equation by iterative methods efficient preconditioned techniques are mandatory. This problem will be addressed in another paper. The Table II compares the numerically obtained frequencies from modified BDF-2, central difference schemes and HB. Due to the high quality factor of the quartz crystal the numerically calculated frequencies from HB and modified BDF-2 are identical up to six digits. Also the estimated frequencies of HB and modified BDF are in excellent agreement (Table II)[2].

TABLE II
THE NUMERICALLY CALCULATED FREQUENCIES OF THE LIMIT CYCLE OF THE COLPITTS OSCILLATOR FOR SEVERAL DIFFERENCE SCHEMES AND HARMONIC BALANCE.

	HB	BDF-2	mod. BDF-2	central differences
$\frac{f_0}{\text{MHz}}$	3.000106	2.997734	3.000106	3.001311

[2]For estimating the free-running frequency of oscillators see i.e. [9].

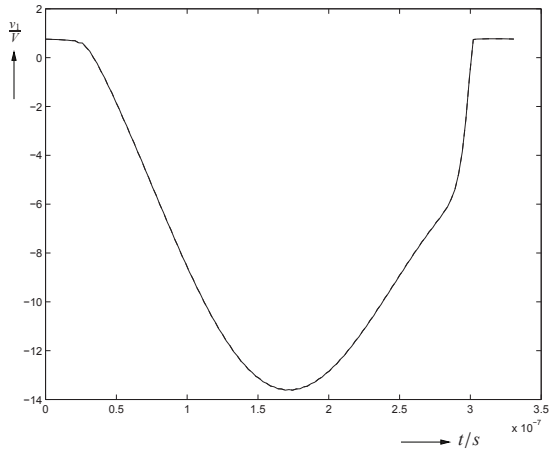

(a) Numerically calculated limit cycle at node 1 of the Colpitts oscillator Fig. 2.

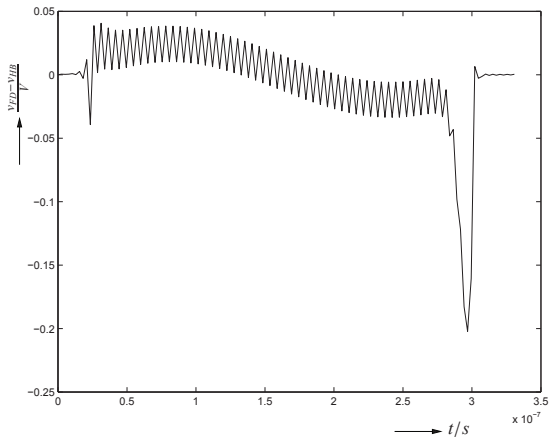

(b) Difference between the Harmonic Balance and the modified BDF scheme solutions.

Fig. 5. Comparison of the numerically calculated limit cycles by the modified BDF scheme of order 2 (dashed) and the Harmonic Balance technique (straight), using 128 grid points per period.

VI. Conclusion

Multistep integration techniques such as the BDF methods are widely used in circuit simulation due to their stiff stability and ease of implementation. However for some circuit classes such as quartz crystal oscillators the BDF techniques lead to erroneous results caused by the numerical damping, which has been studied in detail in this paper. The BDF techniques calculate the exact solution if the waveform is locally a polynomial of degree p. The modified BDF methods proposed here on the other hand calculate the exact solution if the signal waveform is well approximated by a low order trigonometric polynomial. The numerical damping vanishes up to a predefined order of the Fourier series. Simulations obtained from quartz crystal oscillators show excellent agreement with results employing the Harmonic Balance technique, however the sparsity structure is significantly higher and therefore the run-time lower. The investigation of the method for variable step sizes is slightly more complicated due to the fact that the matrices are not circulant. However the approach is equivalent in that case. The truncation error estimation will be considered in another paper.

Acknowledgment

This work has been partly supported by the ENIAC research project ARTEMOS.

References

[1] J. Stoer and R. Bulirsch, *Numerische Mathematik 2*. Berlin: Springer, 1990.

[2] P. Deuflhard and F. Bornemann, *Numerische Mathematik II: Integration gewöhnlicher Differentialgleichungen*. New York: de Gruyter, 1994.

[3] L. O. Chua and P.-M. Lin, *Computer-Aided Analysis of Electronic Circuits: Algorithms and Computational Techniques*. Englewood Cliffs, N. J.: Prentice-Hall, 1975.

[4] C. W. Gear, *Numerical Initial Value Problems in Ordinary Differential Equations*. Englewood Cliffs, N. J.: Prentice-Hall, 1971.

[5] E. Hairer and G. Wanner, *Solving Ordinary Differential Equations II: Stiff and Differential-Algebraic Problems*, ser. Springer Series in Computational Mathematics. Springer, 2010.

[6] A. Brambilla and D. D'Amore, "The simulation errors introduced by the spice transient analysis," *Circuits and Systems I: Fundamental Theory and Applications, IEEE Transactions on*, vol. 40, no. 1, pp. 57–60, Jan 1993.

[7] A. Brambilla and G. Storti-Gajani, "Frequency warping in time-domain circuit simulation," *Circuits and Systems I: Fundamental Theory and Applications, IEEE Transactions on*, vol. 50, no. 7, pp. 904–913, July 2003.

[8] T. Rahkonen and P. Andreani, "Numerical effects in time-domain simulations of electronic circuits - a reminder," *NORCHIP Conference, 2005. 23rd*, pp. 28–31, Nov. 2005.

[9] H. G. Brachtendorf, "Theorie und Analyse von autonomen und quasiperiodisch angeregten elektrischen Netzwerken. Eine algorithmisch orientierte Betrachtung," Universität Bremen, 2001, Habilitationsschrift.

[10] E.-H. Horneber, *Simulation elektrischer Schaltungen auf dem Rechner*. Berlin: Springer, 1985.

[11] J. V. K. Singhal, *Computer Methods for Circuit Analysis and Design*. Springer-Verlag, 1993.

[12] K. E. Brenan, S. L. Campbell, and L. R. Petzold, *Numerical solution of initial-value problems in differential-algebraic equations*. Philadelphia: SIAM, 1996.

[13] W. Kampowsky, P. Rentrop, and W. Schmidt, "Classification and numerical simulation of electric circuits," *Surv. Math. Ind.*, vol. 2, pp. 23–65, 1992.

[14] M. Günther and U. Feldmann, "The DAE-Index in Electric Circuit Simulation," *Mathematics and Computers in Simulation*, vol. 39, pp. 573–582, 1995.

[15] ——, "CAD-based electric-circuit modeling in industry I. Mathematical structure and index of network equations," *Surv. Math. Ind.*, vol. 8, pp. 97–129, 1999.

[16] ——, "CAD-based electric-circuit modeling in industry II. Impact of circuit configurations and parameters," *Surv. Math. Ind.*, vol. 8, pp. 131–157, 1999.

[17] C. Tischendorf, "Topological index calculation of differential-algebraic equations in circuit simulation," *Surv. Math. Ind.*, vol. 8, pp. 187–199, 1999.

[18] W. Gautschi, "Numerical integration of ordinary differential equations based on trigonometric polynomials," *Numerische Mathematik*, vol. 3, pp. 381–397, 1961.